

Ionization-induced gas transparency at the resonant laser action

N.I. Kosarev and N.Ya. Shaparev¹

Siberian Law Institute of the Ministry of the Interior of Russia, Krasnoyarsk

¹*Krasnoyarsk Scientific Center, Siberian Branch of the Russian Academy of Sciences, Krasnoyarsk*

Received December 12, 2005

A radiation-collisional model of the resonant gas ionization by laser has been constructed assuming radiation transfer conditions. A numerical algorithm of solving the problem has been developed for the case of cylindrical geometry of a medium. It was established, that free electrons are formed due to associative ionization. Then the electrons heat up at the second-kind collisions and ionize atoms when colliding. The effect of resonant radiation (with $\lambda = 589.6$ nm) transfer on the kinetics of sodium vapor clearing under ionization-caused clearing-up has been studied for the case of ionizing atoms by an electron avalanche.

Introduction

Gas ionization mechanism based on superelastic heating of electrons has been first proposed in Ref. 1. Then explanation has been given^{2,3} to the results of an experiment,⁴ in which complete sodium-vapor ionization has been obtained at a moderate laser radiation intensity. Under strong photoexcitation of the resonance transition in sodium atoms ($\lambda = 589$ nm) seed electrons appear due to associative ionization.^{1–3} They are quickly heated up due to collisions of the second kind deactivating the excited atoms, and cause the avalanche ionization of the medium due to collisions with them. Such a plasma-forming process has been taken a basis for the radiation-collisional model^{5–6} in which the radiation transfer was neglected. At a large optical density of the medium the secondary radiation significantly changes the excitation kinetics and dynamics of the ionization clearing-up of the gas. The aim of this work was to study numerically kinetics of resonant ionization-caused clearing-up of sodium vapor for the transition at $\lambda = 589.6$ nm under conditions of radiation transfer.

1. Statement of the problem

The mechanism of gas ionization due to superelastic heating, proposed in Refs. 1–3, is applicable to a number of atoms of alkaline and alkaline-earth elements (Li, Na, K, Ba, Mg, etc.). It is needed that for each element one has to construct its own system of levels, in which the number of levels depends on the radiation-collisional properties of the atom. Consider an n -level atom model. Let us denote its ground state by index 1 and the excited one by 2. Let we affect the atom's resonance transition by a laser pulse. Assume atoms to be vaporized inside a cylindrical cell. The problem has been described by balance equations with regard to the following processes: photoexcitation,

photoquenching, and spontaneous decay; electron-impact excitation and deexcitation; associative ionization of the level 2 and electron-impact atom ionization; photo- and three-body recombination.

Equations of the energy level population at a preset medium point r at a time t have the following form:

$$\frac{\partial N_1}{\partial t} = -P_{12}N_1 + P_{21}N_2 + \sum_{i=2}^n A_{i1}N_i + \sum_{i=1}^n (K_{i1}N_i - K_{1i}N_1)N_e + R_1N_e^3 - S_1N_1N_e + F_1N_e^2, \quad (1)$$

$$\frac{\partial N_2}{\partial t} = P_{12}N_1 - P_{21}N_2 + \sum_{i=3}^n A_{i1}N_i - A_{21}N_2 + \sum_{i=2}^n (K_{i2}N_i - K_{2i}N_2)N_e + R_2N_e^3 - S_2N_2N_e + F_2N_e^2 - \alpha_A N_2^2, \quad (2)$$

$$\frac{\partial N_m}{\partial t} = \sum_{i>m} A_{im}N_i - \sum_{i<m} A_{mi}N_m + \sum_{i=m}^n (K_{im}N_i - K_{mi}N_m)N_e + R_mN_e^3 - S_mN_mN_e + F_mN_e^2, \quad m=3, 4, \dots, n, \quad (3)$$

$$\frac{\partial N_e}{\partial t} = \sum_{i=1}^n (S_iN_iN_e - R_iN_e^3 - F_iN_e^2) + \alpha_A N_2^2. \quad (4)$$

Here $N_m(r, t)$ is the concentration of atoms in the m th state; $N_e(r, t)$ is the electron concentration; P_{12} and P_{21} are the frequencies of the radiation photoexcitation and photoquenching of the excited levels of a resonant line

$$P_{12} = B_{12}J(r, t) \text{ and } P_{21} = B_{21}J(r, t) + A_{21},$$

where B_{12} , B_{21} , and A_{21} are the Einstein coefficients for the probability of excitation, stimulated quenching, and spontaneous decay of the level 2; $J(r, t)$ is the radiation intensity integral over solid angles and frequency at the point r of the medium at a time t ; K_{mi} and K_{im} are the coefficients of electron excitation and deexcitation of the levels; S_m is the

coefficient of electron-impact atom ionization from the correspondent states m ; R_m is the three-body recombination rate constant; F_m is the photorecombination coefficient; and α_A is the associative ionization rate constant.

The initial conditions for Eqs. (1) to (3) are as follows:

$$N_1(r, 0) = N_0, \quad N_m(r, 0) = 0, \quad m = 2, 3, \dots, n.$$

They reflect the situation that at $t = 0$ all atoms are in the ground state with the concentration N_0 .

For the electron temperature T_e one can obtain the following equation:

$$\begin{aligned} \frac{\partial T_e}{\partial t} = & \frac{2}{3} \sum_{i>k}^n (K_{ik}N_i - K_{ki}N_k) \Delta E_{ki} + \\ & + \sum_{i=1}^n \left(\frac{2}{3} J_i + T_e \right) (R_i N_e^2 - S_i N_i) - \frac{2}{3} H_{ea} \sum_{i=1}^n N_i - \frac{2}{3} H_{ei} N_e(r, t), \end{aligned} \quad (5)$$

where J_i are the ionization potentials from the corresponding levels; ΔE_{ki} is the energy difference between k and i -levels; H_{ea} and H_{ei} are the rates of energy transfer under elastic collisions of electrons with atoms and ions.

The initial conditions for Eqs. (4) and (5) have the following form:

$$N_e(r, 0) = 0; \quad T_e(r, 0) = T_e^0.$$

Here T_e^0 is the initial temperature of electrons, which are formed due to associative ionization.

The coefficients P_{12} and P_{21} in Eqs. (1)–(4) account for radiation transfer, $J(r, t)$ is determined as

$$J(r, t) = \int_0^{2\pi} d\varphi \int_0^\pi \sin(\theta) d\theta \int_0^\infty \Phi(\nu) I(r, \theta, \varphi, \nu, t) d\nu. \quad (6)$$

The absorption line profile $\Phi(\nu)$ has been represented by the Doppler function of frequency

$$\Phi(\nu) = \frac{1}{\sqrt{\pi}} [\exp(-(\nu - \nu_0)^2 / \Delta\nu_D^2)],$$

where ν_0 is the band center of a spectral line and $\Delta\nu_D$ is its Doppler width. The dependence of the radiation intensity $I(r, \theta, \varphi, \nu, t)$ on the frequency ν , angular θ and φ , and spatial $r(x, y, z)$ variables has been determined from the steady-state transfer equation

$$\frac{\partial I(r, \theta, \varphi, \nu, t)}{\partial l} = \Phi(\nu) \chi_0(N_1, N_2) [S(N_1, N_2) - I(r, \theta, \varphi, \nu, t)], \quad (7)$$

where ∂l is the infinitesimal increment of a photon path along an arbitrary direction \mathbf{L} ; χ_0 is the absorption coefficient at the line center; and S is the source function.

At a complete frequency mixing and spherical scattering phase function of photons, χ_0 and S can be written as follows:

$$\begin{aligned} \chi_0(N_1, N_2) = & \frac{c^2 A_{21} g_2}{8\pi \nu_0^2 g_1} \left[N_1 - \frac{g_1}{g_2} N_2 \right]; \\ S(N_1, N_2) = & \frac{2h\nu_0^3 g_1}{c^2 g_2} \frac{N_2}{N_1 - \frac{g_1}{g_2} N_2}. \end{aligned} \quad (8)$$

Here c is the speed of light; h is the Planck's constant; g_1 and g_2 are the statistical weights of the states 1 and 2, respectively.

Laser radiation has been incident normally to the end plane of the cylinder of the height H_0 . Therefore, the boundary condition for Eq. (7) has the form

$$I(r(Z = -H_0/2), \theta, \varphi, \nu, t) = \begin{cases} 0, & \text{if } \theta \neq 0, \\ I_1(R, \nu, t), & \text{if } \theta = 0 \end{cases} \quad (9)$$

at its left-hand boundary ($Z = -H_0/2$) and

$$I(r(Z = H_0/2), \theta, \varphi, \nu, t) = 0 \quad \text{for } \theta \geq 90^\circ \quad (9a)$$

at its right-hand boundary ($Z = H_0/2$). Here θ is the angle between the direction of a scattered photon propagation and the symmetry axis of the cylinder. Axes of the laser beam and of the cylinder have coincided. The frequency and time dependence of laser radiation has been set by the equation

$$\begin{aligned} I_1(R, \nu, t) = & I_0 \frac{(\Delta\nu/2)^2}{(\nu - \nu_0)^2 + (\Delta\nu/2)^2} \frac{t}{\tau_p} \times \\ & \times \exp\left(1 - \frac{t}{\tau_p}\right) F(R), \end{aligned} \quad (10)$$

where $R(X, Y)$ is the radial coordinate; $F(R)$ is the model function for laser beam intensity versus R ; τ_p is the pulse duration parameter; I_0 is the peak intensity; $\Delta\nu$ is the bandwidth of laser radiation with Lorentzian frequency characteristic.

Numerical algorithm for solving Eqs. (1) to (10), accounting for radiation transfer within a cylinder, is based on the methods that have been developed for the three-level model of sodium atom, considering $3S_{1/2}$, $3P_{1/2}$, and ionization states.⁷ Equations for radiation-collisional coefficients and a technique for their calculation can be found in Ref. 7 as well.

2. Results obtained by numerical modeling

Let us discuss some results on modeling the kinetics of sodium vapor clearing-up at the resonance transition $3S_{1/2} \leftrightarrow 3P_{1/2}$, at the wavelength $\lambda = 589.6$ nm. The atom model included 8 levels, i.e., $3S_{1/2}$, $3P_{1/2}$, $3P_{3/2}$, $4S$, $3D$, $4P$, $5S$, and ionization state.

Calculations were carried out for different parameters of the model: initial concentration N_0 , intensity and duration of laser radiation. The pulse intensity dependence on the transverse coordinate R

altered its form: $F(R) = 1$ for uniform intensity distribution and $F(R) = \exp[-(R/R_b)^2]$ for a Gaussian beam, where R_b is the characteristic beam size. The cylinder height H_0 was equal to 1.0 cm and radius $R_0 = 0.5$ cm.

Dynamics of the electron temperature, electron density, and population of the ground and resonance levels are shown in Fig. 1 for $\tau_p = 2 \mu\text{s}$, $\Delta\nu = 4\Delta\nu_0$, and $I_0 = 10^4 \text{ W/cm}^2$.

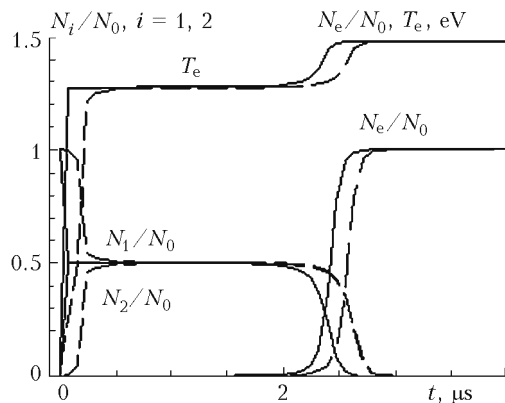


Fig. 1. Dynamics of the electron temperature, electron density, and populations of the ground and resonance states of the sodium atom.

The atom concentration $N_0 = 3.56 \cdot 10^{14} \text{ cm}^{-3}$ corresponded to vapor temperature of 562 K, at which the medium optical depth $\tau_0 = 2880$ along the diameter of the cylinder's base at the line center. Solid curves were obtained for an irradiated end plane at the point corresponding to the axis $Z = -H_0/2$, dashed lines – for the axial point at the shadow end plane $Z = H_0/2$. For such parameters of the model the level populations are close to the saturation ones ($N_1 \cong N_2 \cong 0.5$), so, the high saturation can be achieved with a laser pulse. Free electrons accumulate energy up to $T_e \approx 1.27 \text{ eV}$ due to superelastic processes; then the energy remains unchanged until the avalanche electron ionization of atoms develops. In this situation the population of the resonance (Fig. 1) and other excited levels falls down, by $t > 2.0 \mu\text{s}$, due to a decrease in the number density of atoms. At the stage of electron avalanche the temperature of electrons rises up to 1.46 eV. The balance of direct and reverse exciting collisions of electrons with atoms determines the stationary value $T_e \approx 1.27 \text{ eV}$. The number density of atoms in the transient state decreases; electrons are heated up at quenching the excited level $3^2P_{1/2}$, whose population is maintained by laser radiation and exceeds that of all other levels. After all the atoms have been ionized, the electron temperature goes stabilized again.

Slowing-down of the dynamics of populating the $3^2P_{1/2}$ state and energy accumulation by electrons at the shadow end plane of the cylinder (dashed lines in Fig. 1) is observed at $t < 0.5 \mu\text{s}$. This is explained by laser radiation absorption at an initial stage of the

process, when radiation intensity is yet insufficient for photoexcitation of the $3^2P_{1/2}$ state whose quenching causes the electron heating. The delay in kinetics of N_1 , N_2 , T_e and N_e is due to decelerating of the electron avalanche when propagated from the irradiated end plane of the cylinder to the shadow one (compare dashed and solid lines in Fig. 1).

The radiation transfer through sodium vapor being ionize has been studied assuming uniform intensity distribution over the laser beam cross section. The following features were observed. It is easier for photons to escape from a medium through the envelope of a cylindrical volume, which decreases the number of excited atoms there. Therefore, temperature of electrons near the boundaries is lower than inside the volume, where trapping of radiation provides for maintaining the state with high density of excited atoms (surfaces 1 and 2 in Fig. 2b). Decrease of the electron temperature near the side planes results in less intense atom ionization by electron collisions (surfaces 1 and 2 in Fig. 2a).

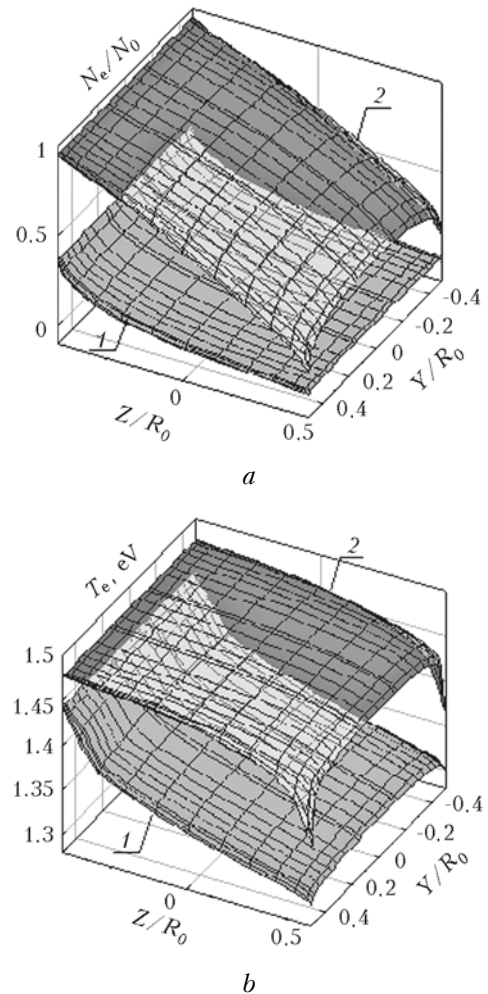


Fig. 2. Spatial distribution of electron density (a) and electron temperature (b) at the time $t = 2.4$ (1) and $t = 2.56 \mu\text{s}$ (2). Parameters of the model correspond to those in Fig. 1.

Calculated data have shown that the laser pulse of intensity $I_0 \leq 10^3 \text{ W/cm}^2$ is strongly absorbed while propagating in a medium. Therefore, ionization does not develop near the shadow end plane of the cylinder. Hence, the radiation transfer results in nonuniform vapor-volume atom ionization because of the electron cooling due to laser radiation absorption and escape of photons from the cylinder.

Studying the laser intensity distribution over the Z-coordinate of the cylinder in different time has pointed out that the laser radiation front goes backward to the irradiated end of cylinder as the electron avalanche develops. This effect of gas darkening has been theoretically predicted in Ref. 8; it is explained by quenching of the excited state by electrons. As a result, the absorption coefficient increases. Then the medium is cleared up again and the laser intensity front moves toward the shadow end of the cylinder when the ionization rate exceeds the rate of collisional quenching.

Figure 3 shows the shapes of input and output laser pulses for different values of the initial atom concentration. Clearing up of the vapor and recovery of the pulse shape (curves 2 and 3) to that of the input pulse (curve 1) are related to the development of ionization. Such a pulse behavior is an evidence of the fact that energy absorbed by vapor should decrease at the vapor ionization.

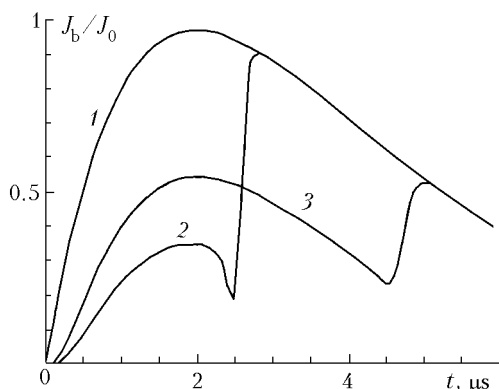


Fig. 3. Time dependences of laser radiation for different initial atom concentrations N_0 : 1 is the input pulse, 2 is the shape of the output pulse for $N_0 = 3.56 \cdot 10^{14} \text{ cm}^{-3}$, and 3 is the output pulse for $N_0 = 1.96 \cdot 10^{14} \text{ cm}^{-3}$. Pulse parameters correspond to those in Fig. 1.

Kinetics of plasma channeling has been calculated by the model, which uses a Gaussian beam. According to the results obtained, the photon transfer from the pumped volume to the radiation-free vapor zone causes an essential increase of the volume with high density of the excited atoms. Its radius is much greater than the beam radius R_b . The density of excited atoms decreases near the cylinder wall due to escape of photons from the medium. Clearing up of the gas due to electron-impact atom ionization begins in the laser beam channel. Electron avalanche forms in the layers, which are close to the irradiated end of the cylinder. Then it propagates deep into the medium providing for additional

ionization-induced clearing up of sodium vapor in the laser beam channel. Thus, a gradual ionization of the laser beam channel occurs.

Along with ionization-caused clearing up of sodium vapor, significant extension of the ionized volume takes place in the laser beam channel. The characteristic size of the plasma channel is much greater than the laser beam size R_b . Strong excitation of the near-channel zone is caused by photon transfer along the cylinder radius and results in free electrons, which then increase their energy in superelastic collisions. Then, as the electron avalanche is initiated in the beam channel, the atom ionization by the electron impact develops outside the channel, as well. Hence, radiation transfer from excitation zone to periphery leads to strong photoexcitation of the medium outside the laser beam. As a result, the ionized volume significantly increases.

Besides the kinetics of populations, the developed algorithm allows one to calculate parameters of the secondary radiation scattered by vapor as a function of frequency, angular, and spatial variables at any specified moment in time. Figure 4 shows the dynamics of the integral, over the laser line, intensity of radiation, scattered by the vapor along different directions, on the path coming through the cylinder center.

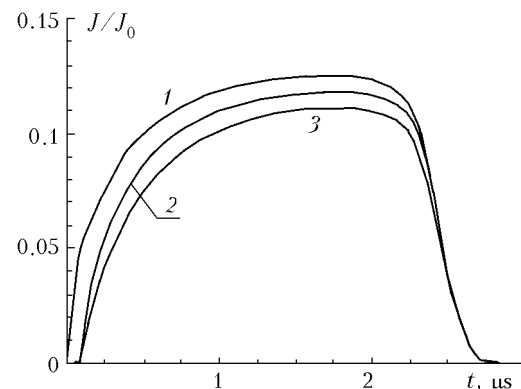


Fig. 4. Dynamics of the frequency-integrated intensity of radiation scattered along different directions θ : curve 1 corresponds to $\theta = 180^\circ$ (backward); curve 2 – 90° ; curve 3 – 0° (forward). Optical paths run through the cylinder center. Pulse parameters correspond to those in Fig. 1; $N_0 = 3.56 \cdot 10^{14} \text{ cm}^{-3}$.

Before the development of the avalanche electron ionization of atoms, the intensity of “backward” scattering (to the angle of 180°) exceeds intensities of scattering along all other directions. It can be explained by an increase of the absorption coefficient of radiation, which propagates inside the medium toward the shadow end of the cylinder. On the contrary, the absorption coefficient for photons, which propagate along the direction opposite to that of the laser pulse, decreases. Therefore, the probability of photon escape to angles close to 180° is greater than those for other scattering angles. Intensities of scattering along all the optical paths

take close values, as the electron avalanche develops, because of the drop of the number of atoms in the volume.

Conclusion

The physical and mathematical model of kinetics of the excitation and ionization of multilevel atoms was constructed with the account for the transfer of resonance radiation. Numerical method of solution of the obtained set of integro-differential equations was developed for cylindrical geometry of the medium. Algorithm for numerical solution of the problem allowed one to calculate plasma-forming kinetics as well as spatial distribution of atomic state populations and electron temperature. Frequency-angular and spatial characteristics were calculated by the transfer equation for each moment in time.

Calculations were carried out for atomic sodium vapor (laser pulse effect on the resonance transition $3S_{1/2} \leftrightarrow 3P_{1/2}$, at the wavelength $\lambda = 589.6$ nm has been modeled). Numerical results showed that radiation transfer results in spatially nonuniform vapor ionization. The concentration of excited atoms as well as electron temperature and concentration are higher inside the volume due to trapping effects. Near the medium boundary, where photon escape is easier, the decay of the excited state results in the electron cooling and in a decrease of the ionization degree.

Absorption of photons scattered within cylinder along the radial directions out of the laser beam

results in strong photoexcitation of the near-channel zone. Here free electrons are produced, which increase their energy due to superelastic impacts and initiate the ionization by electron avalanche. As a result, the ionized volume of the medium significantly increases.

Angular anisotropy and spatial nonuniformity are characteristic of the secondary radiation intensity. Time dependence of the frequency-angular and spatial patterns of vapor luminescence is determined by the dynamics of the ionization transparency. The energy absorbed by vapor drops under conditions of electron ionization. This can be a solution to the problems of effective transport of pulsed laser radiation to the matter.

References

1. R.M. Measures, *J. Appl. Phys.* **48**, No. 7, 2673–2675 (1977).
2. N.Ya. Shaparev, in: *Abstracts of 4th Europhysics Sectional Conference on Atomic and Molecular Physics of Ionized Gases*, Essen (1978), Pt. 48, 120 pp.
3. N.Ya. Shaparev, *Zh. Tekh. Fiz.* **49**, 2229–2231 (1979).
4. T.B. Lucatorto and T.J. McIlrath, *Phys. Rev. Lett.* **37**, No. 7, 428–432 (1976).
5. A.P. Gavriluk and N.Ya. Shaparev, *Opt. Commun.* **39**, No. 6, 379–382 (1981).
6. A.P. Gavriluk and N.Ya. Shaparev, “*Gas ionization in resonance optical field*,” Preprint No. 15, CC SB RAS, Novosibirsk (1986), Part 1, 36 pp.
7. N.I. Kosarev, *Mat. Model.* **17**, No. 5, 105–122 (2005).
8. N.Ya. Shaparev, *Zh. Eksp. Teor. Fiz.* **80**, 957–963 (1981).